
Imaging of Gene Expression in Live Pancreatic Islet Cell Lines Using Dual-Isotope SPECT

Joo Ho Tai¹, Binh Nguyen¹, R. Glenn Wells², Michael S. Kovacs¹, Rebecca McGirr¹, Frank S. Prato¹, Timothy G. Morgan³, and Savita Dhanvantari¹

¹Lawson Health Research Institute, London, Ontario, Canada; ²University of Ottawa Heart Institute, Ottawa, Ontario, Canada; and ³Preclinical Imaging, GE Health Care–Biosciences, London, Ontario, Canada

We are combining nuclear medicine with molecular biology to establish a sensitive, quantitative, and tomographic method with which to detect gene expression in pancreatic islet cells *in vivo*. Dual-isotope SPECT can be used to image multiple molecular events simultaneously, and coregistration of SPECT and CT images enables visualization of reporter gene expression in the correct anatomic context. We have engineered pancreatic islet cell lines for imaging with SPECT/CT after transplantation under the kidney capsule. **Methods:** INS-1 832/13 and α TC1-6 cells were stably transfected with a herpes simplex virus type 1–thymidine kinase–green fluorescent protein (HSV1-thymidine kinase-GFP) fusion construct (tkgfp). After clonal selection, radiolabel uptake was determined by incubation with 5-¹³¹I-iodo-1-(2-deoxy-2-fluoro- β -D-arabinofuranosyl)uracil (¹³¹I-FIAU) (α TC1-6 cells) or ¹²³I-FIAU (INS-1 832/13 cells). For the first set of *in vivo* experiments, SPECT was conducted after α TC1-6/tkgfp cells had been labeled with either ¹³¹I-FIAU or ¹¹¹In-tropolone and transplanted under the left kidney capsule of CD1 mice. Reconstructed SPECT images were coregistered to CT. In a second study using simultaneous acquisition dual-isotope SPECT, INS-1 832/13 clone 9 cells were labeled with ¹¹¹In-tropolone before transplantation. Mice were then systemically administered ¹²³I-FIAU and data for both ¹³¹I and ¹¹¹In were acquired simultaneously. **Results:** α TC1-6/tkgfp cells showed a 15-fold greater uptake of ¹³¹I-FIAU, and INS-1/tkgfp cells showed a 12-fold greater uptake of ¹²³I-FIAU, compared with that of wild-type cells. After transplantation under the kidney capsule, both reporter gene expression and location of cells could be visualized *in vivo* with dual-isotope SPECT. Immunohistochemistry confirmed the presence of glucagon- and insulin-positive cells at the site of transplantation. **Conclusion:** Dual-isotope SPECT is a promising method to detect gene expression in and location of transplanted pancreatic cells *in vivo*.

Key Words: gene expression; pancreatic islet cell transplantation; diabetes; dual-isotope SPECT

J Nucl Med 2008; 49:94–102

DOI: 10.2967/jnumed.107.043430

Diabetes results from the progressive destruction of the insulin-producing β -cells of the pancreatic islet. Treatments for diabetes range from drugs that increase insulin secretion and sensitivity, to insulin administration, to pancreatic islet transplantation. Currently, biochemical markers such as insulin, glucagon and C-peptide, are the only means of noninvasively assessing disease progression and therapy, and abnormalities in these measurements do not surface until most β -cells have been destroyed. Therefore, there is a critical need to monitor the status of islet function *in vivo* over time, in a noninvasive manner.

Several reports have described imaging islets *in vivo*, using bioluminescence in luciferase-expressing islets (1) and transgenic mice (2), and fluorescence detection of green fluorescent protein (GFP) in transfected islets (3). Transplanted islets can also be detected using contrast-enhanced MRI, through labeling with magnetic nanoparticles (4,5) or gadolinium chelates (6), and may prove to be more suitable for long-term monitoring of islet status. In contrast, nuclear medicine techniques may provide a highly sensitive and quantitative means to assess rapid changes in molecular events *in vivo* due to the short half-lives of the isotopes used and detection efficiency. Engineering cells with reporter genes to retain radioisotopes is an approach that has been used to detect gene expression *in vivo* in tumors and stem cells using SPECT and PET. The reporter gene most widely used for PET molecular imaging encodes the viral enzyme, herpes simplex virus type 1 thymidine kinase (HSV1-TK) (7). The most commonly used substrate for HSV1-TK is the pyrimidine nucleoside, 5-iodo-1-(2-deoxy-2-fluoro- β -D-arabinofuranosyl)uracil (FIAU). The HSV1-TK phosphorylates radiolabeled FIAU, thus retaining it in the cell, and the resulting accumulation of the radioactive probe can be imaged by SPECT or PET. Transplanted pancreatic islets expressing TK can be imaged with PET (8), and this approach can be used to image improved islet graft survival after transplantation under the kidney capsule in nonobese diabetic mice (9).

One advantage to using SPECT over PET is the potential to probe multiple molecular mechanisms simultaneously by detecting isotopes with different emission energies

Received May 9, 2007; revision accepted Oct. 1, 2007.
For correspondence or reprints contact: Savita Dhanvantari, PhD, Lawson Health Research Institute, 268 Grosvenor St., London, Ontario N6A 4V2, Canada.
E-mail: sdhanvan@uwo.ca
COPYRIGHT © 2008 by the Society of Nuclear Medicine, Inc.

(10). Recently, our group has developed a method to use multiisotope SPECT for detection of gene expression, cell location, and perfusion to assess the effects of stem cell therapy in a large animal model of myocardial infarct (11). In dogs harboring bone marrow-derived mesenchymal cells expressing HSV1-TK, they were able to simultaneously detect gene expression with ^{131}I -FIAU, verify the location of the stem cell transplants with ^{111}In , and assess the effects of stem cell transplantation on myocardial perfusion with $^{99\text{m}}\text{Tc}$ -sestamibi (11).

We have used the multiisotope detection capabilities of SPECT to simultaneously image the location of, and reporter gene expression in, transplanted pancreatic islet cells in vivo. Two studies were conducted: one in which SPECT images were collected with a single-head γ -camera and coregistered with CT to localize the functional SPECT signals in an anatomic context, and one in which a new scanner with a solid-state cadmium–zinc–telluride (CZT) detector was used for simultaneous acquisition of 2 isotopes. Our results show that the simultaneous in vivo imaging of pancreatic islet gene expression and location is possible using SPECT.

MATERIALS AND METHODS

Cell Lines and Culture

Two pancreatic islet cell lines were used in this study: the glucagon-secreting $\alpha\text{TC1-6}$ cell line, and the insulin-secreting INS-1 832/13 cell line. The $\alpha\text{TC1-6}$ cells were a generous gift from Dr. C. Bruce Verchere (University of British Columbia). These cells represent a pure population of mature pancreatic α -cells (12) that we have used to study α -cell physiology (13). Wild-type (WT) $\alpha\text{TC1-6}$ cells were cultured in Dulbecco's modified Eagle medium (DMEM) (Invitrogen) containing 4.5 g/L glucose, 15% (v/v) horse serum (HS) (Invitrogen), and 2.5% (v/v) fetal bovine serum (FBS) (Invitrogen). INS-1 832/13 cells were a kind gift from Dr. Chris Newgard (Duke University Medical Center). The parental cell line was originally derived from a rat insulinoma (14), and the 832/13 clone stably expresses the human proinsulin gene and shows glucose-stimulated insulin secretion (15). INS-1 cells were cultured in RPMI 1640 medium (Invitrogen) containing 10 mM *N*-(2-hydroxyethyl)piperazine-*N'*-(2-ethanesulfonic acid) [HEPES], 10% (v/v) FBS, 1 mM sodium pyruvate, and 0.05 mM β -mercaptoethanol.

Constructs and Stable Clone Generation

The plasmid pNES-tkgfp was a kind gift from Juri Gelovani (MD Andersen Cancer Center, University of Texas). WT $\alpha\text{TC1-6}$ cells were transfected with pNES-tkgfp using Lipofectamine 2000 (Invitrogen) as per manufacturer's instructions. Cells were maintained in selection media containing 0.5 mg/mL G418 (Invitrogen) for 2–3 wk. For transfection of INS-1 832/13 cells, the HSV1-tk-gfp fragment was ligated into pcDNA3.1/Zeo+ (Invitrogen). INS-1 832/13 cells were transfected with pcDNA3.1/tkgfpZeo+, and stable clones were selected in media containing 50 $\mu\text{g}/\text{mL}$ Zeocin (Phleomycin D1; Invitrogen) for 2–3 wk. Both $\alpha\text{TC1-6}$ and INS-1 clones were screened for GFP expression by Western blot, as we have done previously (13) using an antibody against GFP (Clontech) at a dilution of 1:1,000. In all constructs, expression of the reporter gene was driven by the constitutive cytomegalovirus promoter.

After antibiotic selection, one clone of $\alpha\text{TC1-6}$ cells expressed GFP in nearly 100% of the cells. However, the selected INS-1 stable clone did not express GFP very efficiently after antibiotic selection; therefore, this clone was further purified with fluorescence-activated cell sorting (FACS). Single-cell suspensions were prepared and filtered through a 40- μm cell strainer (Becton-Dickinson). A suspension of 2×10^7 cells/mL was prepared in phosphate-buffered saline containing 3% FBS for sorting. Cells were sorted for GFP fluorescence and analyzed using a FACSVantage SE DiVa flow cytometer (Becton-Dickinson). The resulting sorted cell population was >99.5% positive for GFP.

Radiolabeled Substrate Synthesis

5-Trimethylstannyl-1-(2-deoxy-2-fluoro- β -D-arabinofuranosyl)uracil (FTAU), FIAU, and 1-(2-deoxy-2-fluoro- β -D-arabinofuranosyl)uracil (FAU) were purchased from ABX Advanced Biochemical Compounds. Sodium ^{131}I -iodide (Perkin Elmer) was obtained without stabilizer added. Sodium ^{123}I -iodide was purchased from MDS Nordion. Disodium hydrogen phosphate, sodium hydroxide, and sodium sulfite (BDH), glacial acetic acid (EM Science), 30% hydrogen peroxide (Fisher Scientific), and helium and nitrogen gas (BOC Gases) were used without further purification. Methanol and chloroform (high-performance liquid chromatography [HPLC] grade; Fisher Scientific) and water (distilled and deionized) were membrane filtered (25 μm) before use.

The preparation of $^{131/123}\text{I}$ -FIAU was accomplished through modification of a published method (16), as follows: To a V-vial equipped with a septum and containing FTAU (25 μg , 0.067 μmol) in 100 μL chloroform and 5 μL of 3:1 (v/v) acetic acid/30% hydrogen peroxide, were added 37–185 MBq sodium $^{131/123}\text{I}$ -iodide in 10–20 μL of 0.1 M sodium hydroxide. After ultrasonication for 5 min, 10 μL 0.2 M sodium thiosulfate was added and the V-vial was purged with nitrogen gas through a charcoal trap. HPLC purification was performed with a Waters Breeze system equipped with a Waters Symmetry 4.6 \times 150 mm C18 column at a flow rate of 1.5 mL/min. The entire volume of the reaction vial was injected and isocratically eluted with 95:5 10 mM disodium hydrogen phosphate/ethanol. Radioactive fractions were detected using a Carroll and Ramsey Associates γ -flow detector model 105S-1. A Capintec CRC-15R dose calibrator was used for radioactivity measurements. Product was obtained with >90% of the radioactivity attributed to the ^{131}I -FIAU peak and with no visible mass peak (<2 nmol). The HPLC product was drawn over a tC18 Sep-Pak column (Waters), eluted with 3.0 mL ethanol, concentrated, and reconstituted in a smaller volume suitable for intravenous injection. Final yields were 20%–80%.

Cellular Uptake of $^{131/123}\text{I}$ -FIAU and ^{111}In -Tropolone

One million $\alpha\text{TC1-6}$ WT and clone 5 cells were plated in a 6-well plate, and incubated in 0.5 mL of media containing 0.185, 0.37, or 1.85 MBq ^{131}I -FIAU for 3 h or 1, 10, or 50 MBq ^{111}In -tropolone for 30 min. After incubation, media were removed, and cells were washed 3 times with chilled Hanks' buffered saline solution ([HBSS] 5.3 mM KCl, 0.44 mM KH_2PO_4 , 0.14 M NaCl, 4.16 mM NaHCO_3 , 0.34 mM Na_2HPO_4 , and 5.55 mM glucose, pH 7.4, containing 2% FBS) and scraped in 1 mL of ice-cold HBSS. The cellular ^{131}I -FIAU and ^{111}In -tropolone uptake was calculated as the percentage of cellular ^{131}I or ^{111}In from the total radioactivity in the media, wash, and cell extracts. For determination of the kinetics of ^{131}I -FIAU uptake, $\alpha\text{TC1-6}$ WT and clone 5 cells were incubated with 0.5 mL media containing 0.185 MBq

^{131}I -FIAU for 30 min and 3, 6, or 19 h. The cellular ^{131}I -FIAU uptake was measured as described above after each incubation period. The rate of ^{131}I -FIAU uptake at each time period was generated using the linear regression method in Microsoft Excel. For in vitro experiments using ^{123}I -FIAU, 2 million INS-1 WT and clone 9 cells were incubated with 7.4 MBq/mL ^{123}I -FIAU for 1 h, and cellular uptake was calculated as described for ^{131}I -FIAU.

Renal Subcapsular Transplantation

All animal procedures were in accordance with the Canadian Council on Animal Care and were approved by the Animal Use Subcommittee of the University of Western Ontario. Male CD1 mice (25–30 g) were purchased from Charles River Laboratories. For the first set of in vivo experiments, one group of WT $\alpha\text{TC1-6}$ cells and clone 5 cells was labeled overnight with 1.85 MBq ^{131}I -FIAU as described. On the morning of surgery, a second group of WT $\alpha\text{TC1-6}$ cells and clone 5 cells was labeled with 20 MBq ^{111}In -tropolone for 30 min. For simultaneous dual-isotope acquisitions, INS-1 clone 9 cells were labeled with only ^{111}In -tropolone as described. Cells were dissociated from the plate and loaded into gel-loading pipette tips in 100 μL of culture media, and the end of the tips were sealed by cauterization. The loaded tips were placed into tubes and centrifuged at 1,100 rpm for 1 min. Mice were anesthetized with inhalable 2% isoflurane through a nose cone throughout the surgery. The left kidney was exteriorized, and a small path for the pipette tip was made using a fine needle. The pipette tip was cut with a sterile razor blade, inserted into the path under the kidney capsule, and cells were infused using a manual syringe pump or 20- μL pipette. The kidney capsule was sealed by cauterization, followed by closure of the skin incision.

SPECT/CT

Two days after cell transplantation, mice were imaged using SPECT. For the duration of all imaging sessions, the mice were kept anesthetized using inhalable 2% isoflurane gas. For the first in vivo study using $\alpha\text{TC1-6}$ clone 9 cells labeled with ^{131}I -FIAU or ^{111}In , SPECT images were obtained using a StarCam 4000i γ -camera (GE Healthcare) equipped with a 1-mm aperture single-pinhole collimator (26-cm focal length). Each mouse was positioned in a custom-built animal rotation platform and rotated in a vertical position in front of the γ -camera. Projection data were acquired as 100 images over 360°, each 256 \times 256 pixels with a pixel size of 1.6 mm. The radius of rotation was 4.9 cm. Data were acquired separately for the ^{131}I and ^{111}In signals. An energy window of 364 keV \pm 10% was used for ^{131}I and the sum of the 245-keV 10% and 173-keV 10% energy windows was used for ^{111}In . Data were acquired for 1–4 h for each animal, depending on the strength of the signal, and then corrected for isotope decay back to the starting time of the study. To assist in coregistration of the SPECT and CT images, 4 fiducial markers were taped to the mouse, and SPECT projection data were acquired for the markers. For ^{131}I acquisitions, the fiducial markers consisted of capillary tubes containing Omnipaque (Iohexol; GE HealthCare) CT contrast material and $^{99\text{m}}\text{Tc}$, with the $^{99\text{m}}\text{Tc}$ acquired in a second scan (with a 126- to 154-keV energy window) after ^{131}I . For ^{111}In acquisition, the capillary tubes contained Omnipaque CT contrast material and ^{111}In , and the ^{111}In was acquired in the same scan.

After SPECT acquisition, the imaging bed was disconnected from the rotation platform and transported to the CT suite without moving the mouse relative to the bed. The imaging bed was positioned horizontally in the CT scanner with care taken to

minimize any movement of the mouse. A helical CT scan of the mouse was then acquired on a Discovery LS PET/CT system (GE Healthcare). The CT field of view was 9.6 cm with a slice thickness of 0.625 mm.

The SPECT images were reconstructed using the ordered-subset expectation maximization (OSEM) iterative algorithm into a 128 \times 128 \times 128 array with an isotropic voxel size of 0.2 mm. Images were then filtered with a 3-dimensional gaussian function having a full width at half maximum of 0.6 mm. These images were registered to the CT images off-line, using in-house software that performed a 6-degree-of-freedom rigid-body transformation, which minimized the distance between the centers of the fiducial markers in the SPECT and CT images.

In the second study, we used simultaneous acquisition dual-isotope SPECT. Mice bearing ^{111}In -tropolone-labeled INS-1 clone 9 cells were injected intravenously with 7.4 MBq ^{123}I -FIAU 1 h before imaging. SPECT images were obtained using a preproduction eXplore speCZT small-animal SPECT scanner (GE Healthcare). The scanner uses a stationary, full ring of CZT detectors for increased scan speed and sensitivity. Additionally, the high-energy resolution of CZT provides the capability of simultaneously imaging multiple radionuclides with close energy spectra. An 8-slit collimator was used with a field of view of 32 and 78 mm in the transaxial and axial directions, respectively. With the full ring detector, 360° of data were acquired by rotating the collimator 45° (15 steps, 3°/step). During acquisition, 300,000 counts per step were acquired in list mode, using an energy window of 51–250 keV. The scan duration was 21 min.

The SPECT images were reconstructed using the OSEM iterative algorithm into a 128 \times 128 \times 32 array with a voxel size of 0.25 \times 0.25 \times 2.46 mm. Reconstructions for ^{123}I and ^{111}In were generated independently. An energy window of 150–165 keV was used for ^{123}I , and the sum of the counts between 166 and 180 keV and 205 and 215 keV was used for ^{111}In . The second ^{111}In peak was detected at 210 keV instead of 245 keV due to the nonlinearity of the detectors above 200 keV. Because of the closeness of the ^{123}I and the first ^{111}In peak, images were also reconstructed using only the second peak of ^{111}In and a narrower window for the ^{123}I peak (157–162 keV). The energy spectrum from the slices containing only the kidney was plotted to examine the amount of downscatter from ^{111}In in the ^{123}I window. Three-dimensional image reconstructions were viewed in MicroView (GE Healthcare) to localize the ^{123}I or ^{111}In signals individually or both simultaneously with different color maps.

Immunohistochemistry

After imaging, kidneys were excised, fixed in 10% neutral buffered formalin for 24–36 h, and embedded in paraffin. Sequential sections of 5 μm were cut and mounted onto SuperFrost Plus glass slides (Fisher Scientific). Slides were incubated for 24 h at 4°C with either mouse antiinsulin (Sigma) or rabbit antiglucagon antiserum (Santa Cruz Biotech) at a dilution of 1:250 and then incubated with biotinylated horse antimouse or goat antirabbit IgG (Sigma-Aldrich) at a dilution of 1:500, as described (17). Peptide immunoreactivity was localized by incubation in fresh diaminobenzidine tetrahydrochloride (Biogenex). Tissue sections were counterstained with Carazzi's hematoxylin.

Statistical Analysis

For all experiments, 1-way ANOVA combined with a post hoc Student *t* test was used to determine the significant differences

between WT cells and clones. The significance was set at $P < 0.05$.

RESULTS

^{131}I -FIAU Uptake in $\alpha\text{TC1-6}$ and INS-1 Clones

Both $\alpha\text{TC1-6}$ cells and INS-1 832/13 cells were stably transfected with tk-gfp and screened for GFP expression by Western blot. Of the 7 $\alpha\text{TC1-6}$ clones selected, 1 clone (clone 5) showed high TK-GFP expression (Fig. 1A). Expression of GFP in both $\alpha\text{TC1-6}$ clone 5 cells was confirmed with fluorescence microscopy in live cells (Fig. 1A). $\alpha\text{TC1-6}$ clone 5 cells retained a 10-fold greater amount of ^{131}I -FIAU ($P < 0.001$), compared with WT and clone 1 (Fig. 1B). In INS-1 832/13 cells stably transfected with tk-gfp, 1 clone (clone 9) was selected on the basis of Western blot analysis of GFP expression. However, these cells initially showed weak GFP fluorescence. Therefore, the GFP-expressing cell population was enriched using FACS (Fig. 2A), and subsequent analysis showed that 100% of the cell population expressed GFP fluorescence (Fig. 2B). Clone 9 cells retained a 12-fold greater amount of ^{123}I -FIAU ($P < 0.001$) compared with WT cells (Fig. 2C).

Cellular uptake of both ^{131}I -FIAU and ^{111}In -tropolone remained relatively constant over a range of concentrations, and the total radioactive burden per cell increased with the

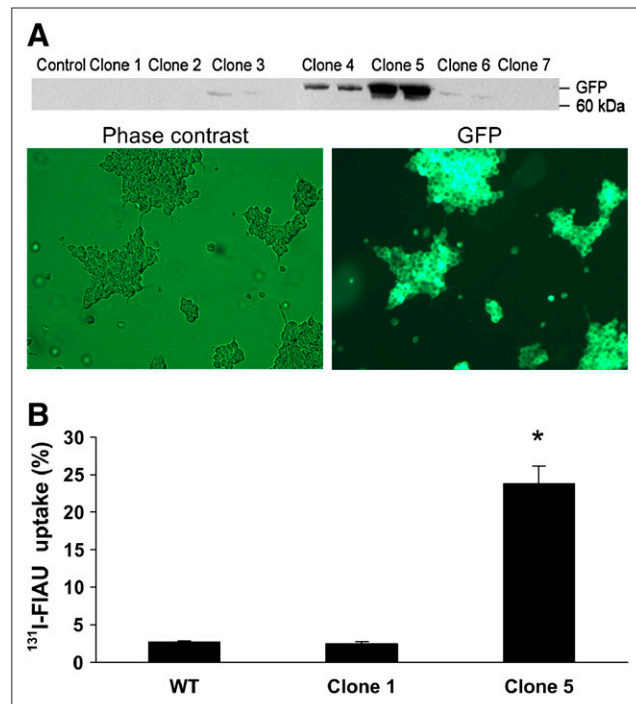


FIGURE 1. (A) $\alpha\text{TC1-6}$ cells were stably transfected with a vector encoding HSV-1 TK and GFP. Clone 5 was chosen on the basis of high expression of GFP by Western blot and fluorescence microscopy. (B) $\alpha\text{TC1-6}$ clone 5 accumulated ^{131}I -FIAU to 14-fold higher levels than low-expressing clones ($P < 0.001$ compared with clone 1 and WT). Values are expressed as mean \pm SEM ($n = 3$).

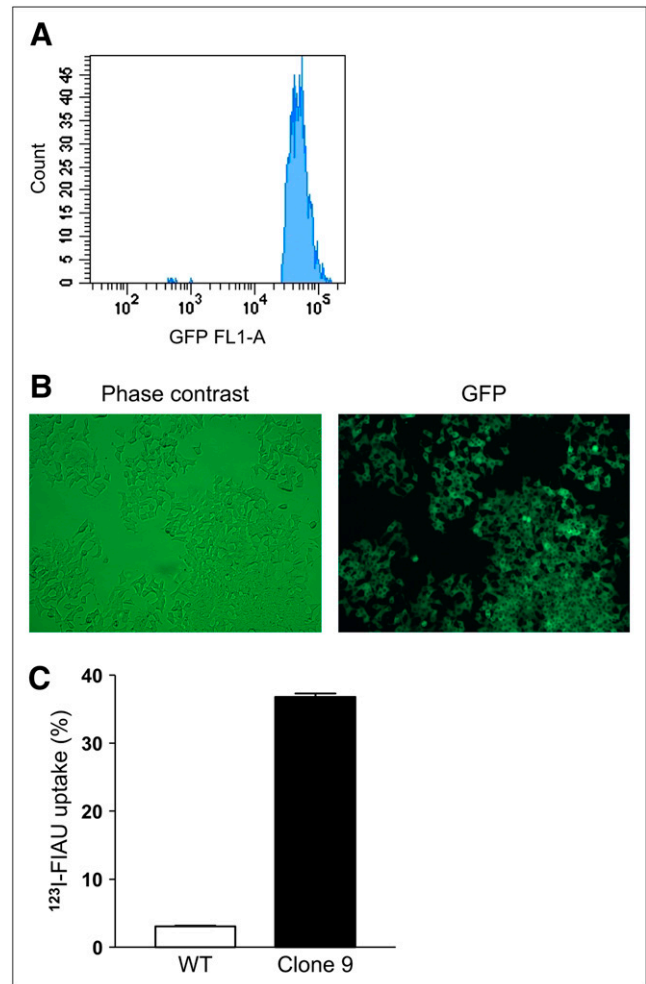


FIGURE 2. (A) INS-1832/13 cells were stably transfected with HSV1-TK-GFP and further selected by FACS as described. (B) Expression of GFP in FACS-sorted clone 9 cells was confirmed by fluorescence microscopy. (C) Clone 9 cells accumulated ^{123}I -FIAU to 12-fold higher levels than WT cells ($P < 0.001$). Values are expressed as mean \pm SEM ($n = 3$).

corresponding increase in concentration in $\alpha\text{TC1-6}$ clone 5 cells (Table 1). No negative effects on cell viability were observed at any of the concentrations listed in Table 1 (data not shown). Accumulation of ^{131}I -FIAU in cells expressing TK-GFP increased over time, with the highest rate of uptake in the first 3 h (data not shown).

Imaging

After engineered $\alpha\text{TC1-6}$ and INS-1 cells were characterized in terms of ^{131}I -FIAU uptake, cells were transplanted for initial in vivo imaging studies. One million $\alpha\text{TC1-6}$ clone 5 cells were incubated with either 1.85 MBq ^{131}I -FIAU or 20 MBq ^{111}In -tropolone and transplanted under the left kidney capsule of CD1 mice. Both the ^{131}I and ^{111}In signals from the transplanted cells could be readily detected in the transaxial slices of the reconstructed SPECT images (Fig. 3A). Anatomic coregistration with the CT image in transaxial slices (Fig. 3A) and reprojected

TABLE 1In Vitro Uptake of ^{131}I -FIAU and ^{111}In -Tropolone in Clone 5 $\alpha\text{TC1-6}$ cells

Radionuclide	Amount (MBq)	% Uptake*	Bq/cell*
^{131}I	0.185	47 ± 0.8	0.09 ± 0.001
	0.37	50 ± 0.4	0.18 ± 0.001
	1.85	52 ± 0.6	0.97 ± 0.01
^{111}In	1	58 ± 1.1	0.58 ± 0.01
	10	59 ± 0.9	5.9 ± 0.1
	50	53 ± 0.4	26.5 ± 0.2

*Data are expressed as mean \pm SEM.

maximum-intensity-projection axial views (Fig. 3B) showed the ^{131}I and the ^{111}In SPECT signals in the appropriate anatomic context. To confirm the specificity of the signal, both kidneys were excised and counted. The left kidneys showed a 491-fold greater amount of ^{131}I per gram tissue than the right kidneys ($P < 0.001$, $n = 3$). Immunohistochemistry showed glucagon staining in the cell grafts in the kidney capsule (Fig. 3C), confirming the location of the transplanted cells. Although serum glucagon levels were not measured, both retention of FIAU and glucagon immunoreactivity indicate that protein synthesis was intact and that the cells remained viable after transplantation.

In a second set of experiments, we detected both gene expression and location simultaneously in INS-1 clone 9 transplants using dual-isotope SPECT. Cells were first labeled with 20 MBq ^{111}In -tropolone for 30 min and transplanted under the left kidney capsule of CD1 mice. Two days after transplantation, mice were injected intravenously with 7.4 MBq ^{123}I -FIAU and, 1 h later, mice were imaged using a preproduction GE Healthcare eXplore speCZT unit. Images for both ^{123}I and ^{111}In were acquired simultaneously over 21 min. Signals for both isotopes colocalized in the site of the transplant in the left kidney (Fig. 4A). There was some ^{123}I in the bladder due to clearance. The images reconstructed with only the second ^{111}In peak showed ^{111}In activity at the site of the transplant in the left kidney. The ^{123}I images reconstructed with a narrower window showed activity locations similar to those of the reconstructions performed with the original window. It is important to note that the energy spectrum generated from kidney slices showed a distinct peak in the ^{123}I window, verifying ^{123}I activity in addition to the downscatter from ^{111}In .

After imaging, mice were sacrificed, and tissue biodistribution of ^{123}I was assessed. Figure 4B shows that ^{123}I significantly accumulated in the left kidney (the site of transplantation). In contrast, the stomach, small and large intestine, gallbladder, and liver did not retain ^{123}I . There was some ^{123}I in the thyroid, most probably due to accumulation to free iodine, and the right kidney, due to clearance. To further confirm that the signal came from

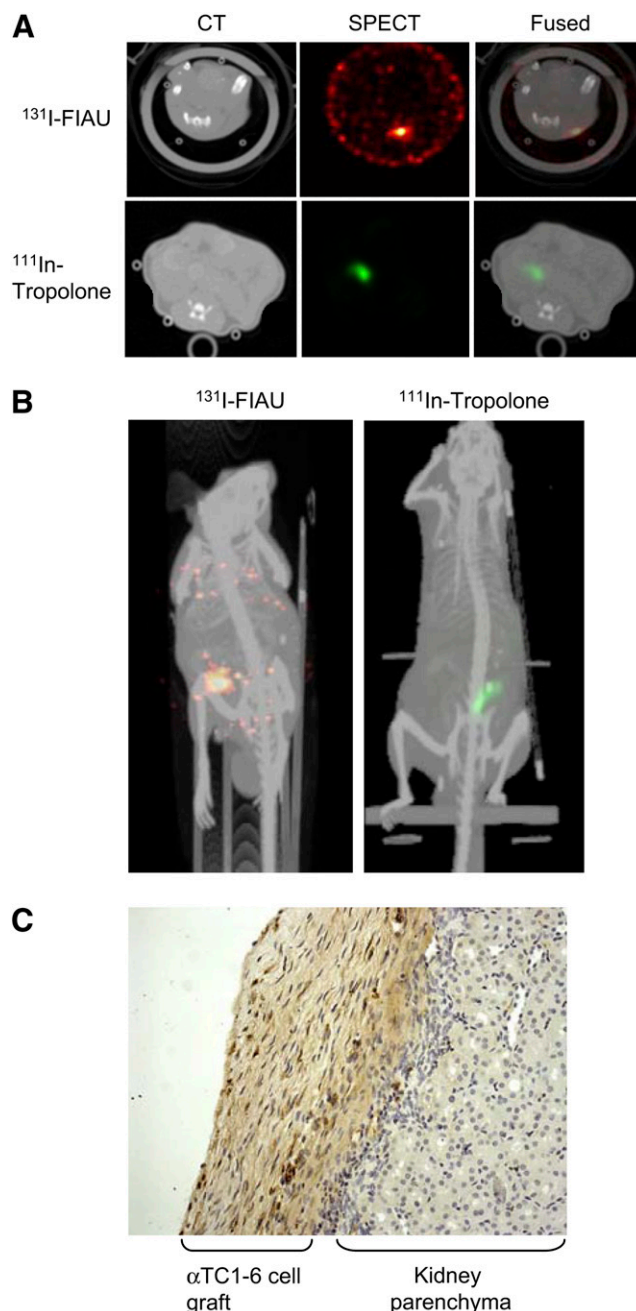


FIGURE 3. In vivo imaging of transplanted cells using SPECT/CT. (A) One million $\alpha\text{TC1-6}$ clone 5 cells were labeled with 1.85 MBq ^{131}I -FIAU or 20 MBq ^{111}In -tropolone and transplanted under the left kidney capsule of CD1 mice. Two days later, SPECT images were acquired using a 1-mm pinhole collimator. CT images were acquired and coregistered with SPECT images. (B) Three-dimensional reconstructions of SPECT/CT images shown in A. (C) Histochemical staining confirms presence of $\alpha\text{TC1-6}$ clone 5 cells by glucagon-positive staining (brown) on kidney parenchyma.

labeled cells, immunohistochemical staining for insulin was conducted on kidney sections. Insulin staining was seen in the kidney capsule (Fig. 4C), confirming the location of the transplanted cells.

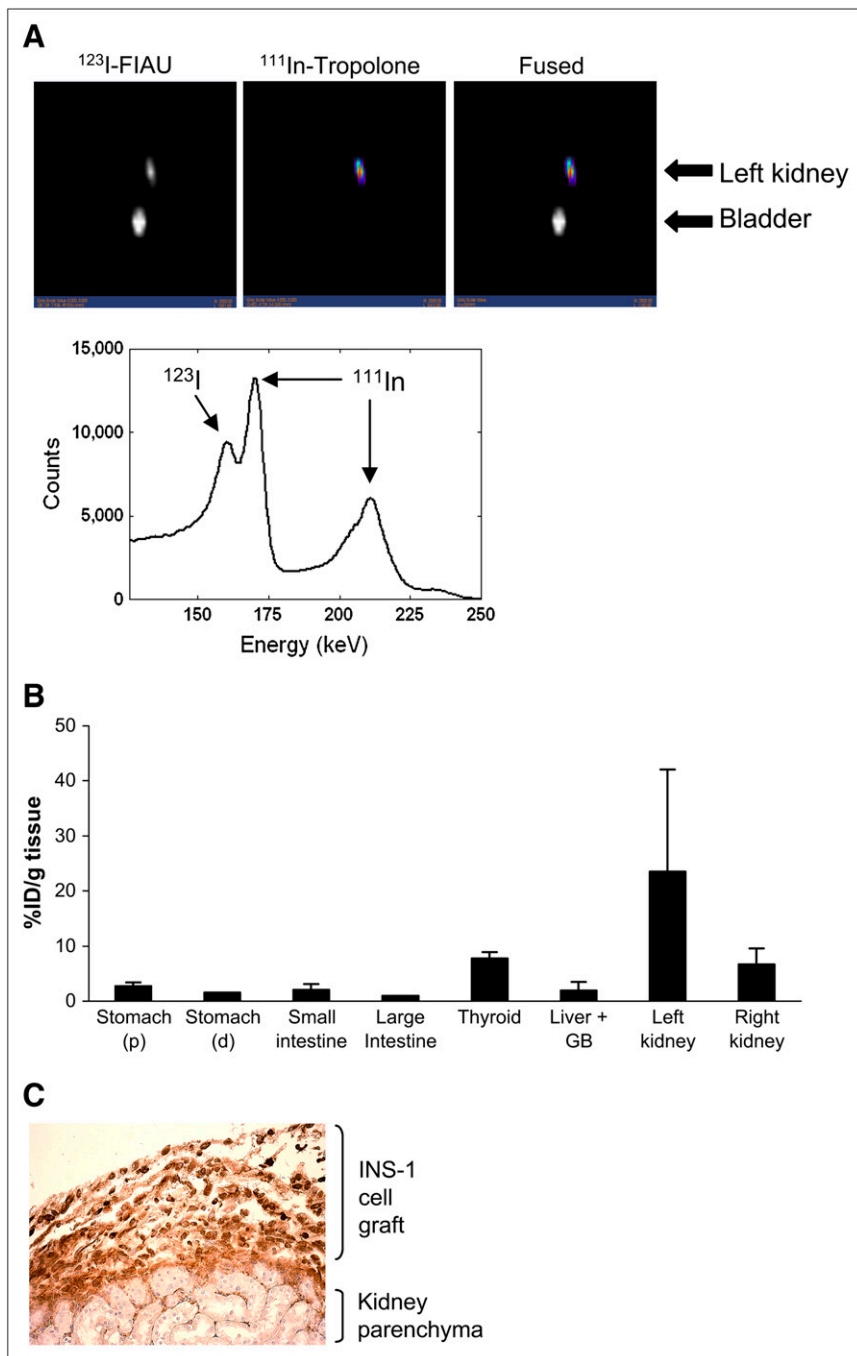


FIGURE 4. (A) Dual-isotope SPECT images of INS-1 832/13 clone 9 cells after transplantation under the kidney capsule of CD1 mice. Cells were labeled with 20 MBq ^{111}In -tropolone before transplantation. Two days after transplantation, mice were systemically administered 7.4 MBq ^{123}I -FIAU. Simultaneous acquisition of both isotope energies shows presence of both isotopes in region of the transplant (left kidney). Energy spectrum from the volume of interest surrounding left kidney shows distinct peaks for ^{123}I and ^{111}In (arrows). (B) Biodistribution of ^{123}I counts was determined after the imaging session. All counts were calculated as percentage injected dose per gram wet tissue weight (%ID/g tissue) and normalized to values in large intestine (tissue with the lowest value). Bars represent mean \pm SEM ($n = 3$). (C) Histochemical staining confirms presence of INS-1 clone 9 cells by insulin-positive staining (brown) on the kidney parenchyma.

DISCUSSION

In vivo imaging of islets and β -cells in particular is a rapidly emerging field of interest, given the rapid rise in the incidence of diabetes globally. The development of more-effective therapies to either maintain the health of transplanted islets or reversing apoptosis in β -cells during the progression of the disease can be accelerated with in vivo imaging modalities. It has been shown that the fate of transplanted islets and cells can be tracked over time using several imaging modalities, such as contrast-enhanced MRI

(4,5), PET (8,9,18), and bioluminescence (2), thus enabling longitudinal studies of disease progression and therapy.

In this study, we have used SPECT/CT and dual-isotope SPECT to track the location of and to detect reporter gene expression in pancreatic islet cell lines that have been engineered for radionuclide retention. In particular, we have stably transfected 2 pancreatic cell lines, α -TC1-6 cells and INS-1 832/13 cells, to express the HSV-1 tk gene, which causes the intracellular retention of a radionuclide probe, ^{131}I -FIAU. The resulting accumulation of ^{131}I -FIAU can be imaged using a γ -camera. Engineered cells can be

imaged after transplantation under the kidney capsule, and the resulting SPECT images can be coregistered with CT to provide an anatomic context for the functional signal. We could also detect transplanted cells with ^{111}In -tropolone, thereby demonstrating the potential of imaging both gene expression and location using dual-isotope SPECT. Engineering islets with the reporter genes hsv-tk for PET (9) or luciferase for imaging by bioluminescence (2,19) is an ideal means to assess islet function in vivo in real time. These studies also showed that reporter gene expression per se does not affect islet architecture or insulin expression, as assessed by immunohistochemistry, and glucose-stimulated insulin secretion is not affected. Although we did not measure serum glucagon or insulin levels in the present study, immunohistochemistry of cell grafts is in agreement with the aforementioned studies, thus showing that engineered transplanted cells are intact and are producing hormone.

Our group has previously used SPECT in a quantitative manner to track transplanted stem cells. By labeling canine bone marrow mesenchymal cells with ^{111}In -tropolone, we have estimated the limit of detection at 3,200 cells, with a radioactive burden of 0.14 Bq per cell (20). Additionally, our group has also shown that application of corrections for Compton scatter, radionuclide crosstalk, and attenuation in SPECT image processing can improve multiisotope detection (11). Therefore, we have shown that multiisotope SPECT can be very sensitive and quantitative. Some common clinical applications of multiisotope SPECT are dual-isotope stress–rest cardiac perfusion imaging with ^{201}Tl -chloride and $^{99\text{m}}\text{Tc}$ -sestamibi (21) or ventilation–perfusion lung imaging with $^{99\text{m}}\text{Tc}$ -macroaggregated albumin and ^{133}Xe gas (22). Dual-isotope SPECT has also been used in a rat model of myocardial infarct to track transplanted stem cells by labeling them with ^{111}In and assessing effects on perfusion with $^{99\text{m}}\text{Tc}$ -sestamibi (23). In this way, the effects of stem cell therapy on reestablishing myocardial perfusion could be simultaneously detected. However, these studies did not engineer transplanted cells for detection of reporter gene expression; therefore, detection was limited to tracking the location of the cells and their effects on the surrounding tissue. Nonetheless, these studies demonstrate that SPECT is sensitive, quantitative, and capable of monitoring multiple cellular events simultaneously. In the present study, we show that this strength of SPECT can be applied to assess both gene expression and location of transplanted pancreatic islet cell lines in vivo. For future longitudinal studies assessing the status of transplanted islets using SPECT, multimodality hybrid imaging, such as SPECT/MRI, would be ideal to image changes in islet gene expression and location of the transplants. Labeling islets with an MR contrast agent may provide a more stable means of monitoring the location of the islets, whereas the short half-lives of SPECT isotopes could be useful in assessing transient changes in molecular events.

Radioisotope labeling of cells may result in reduced survival or function, primarily due to incorporation of the

radiolabel into the DNA. For our in vivo studies, we estimated a radioactive burden of 12 Bq of ^{111}In per cell and 1 Bq of ^{131}I per cell. Several studies have described the effects of ^{111}In on viability in several different cell types. Over a short time period (24 h), viability and proliferation of human hematopoietic progenitor cells (24) or mesenchymal stem cells (25) were not affected by doses similar to those used in the present study. However, over longer periods, viability decreases in a dose-dependent manner (20,26). Therefore, for long-term monitoring of transplants, lower doses of ^{111}In should be used. For ^{131}I , a cell dosimetry assay has defined a maximum tolerable dose of 800 cGy for NIT+ T cells labeled with ^{131}I -FIAU (27). Such an algorithm could conceivably be developed for any isotope used to label cells for imaging and would ensure optimum radiolabeling of cells for SPECT without compromising cell viability or function.

In the present study, the reconstruction algorithm in the dual-isotope acquisitions did not include crosstalk compensation. However, the energy spectrum around the kidney verified separate ^{123}I activity in addition to downscatter from ^{111}In . Future studies may use windowing techniques for crosstalk compensation (28). Additionally, the SPECT and CT images were acquired on 2 separate cameras, in 2 different bed positions, with coregistration of the images being done via fiducial markers. Small shifts of the animal during transport between cameras and during changes in bed position can reduce the accuracy of the CT-based localization. However, newer SPECT/CT systems such as the eXplore speCZT/CT allow acquisition of both SPECT and CT on the same platform, thereby eliminating any serious issues with alignment.

Imaging of HSV1-tk reporter gene expression with the probe 9-(4-[^{18}F -fluoro-3-[hydroxymethyl]butyl]guanine (^{18}F -FHBG) in pancreatic islet transplants has been reported recently. Two studies (8,18) show that transplanted islets infected with viral vectors encoding thymidine kinase could be detected for up to 90 d after transplantation into the axillary cavity. A subsequent study using the same approach showed that improved renal subcapsular graft survival could be detected by PET after coinfection of islets with both tk and a survival factor, interleukin-10 (9). Additionally, evidence was provided that this method could be used to detect intrahepatic islet isografts, thus showing the utility of this approach in a clinically relevant model. Therefore, the reporter gene approach will provide a useful model for devising therapies to improve islet survival after transplantation.

In our system, we have used pancreatic islet cell lines selected for TK expression in lieu of virally transfected islets. Although it can be argued that cell lines are not truly representative of islets, we (13) as well as others (29) have shown that the $\alpha\text{TC1-6}$ cell line can respond to insulin and glucose as effectively as intact α -cells. Likewise, INS-1 832/13 cells have been shown to metabolize glucose and lipids in a manner that mimics β -cells in the intact islet

(15,30). In fact, it has been suggested that insulin-producing cell lines be propagated for transplantation due to the scarcity of organ donors for islet transplantation (31,32). Because of the ease of manipulating and transplanting cell lines, imaging gene expression events in transplanted cell lines could shed some light on β -cell gene regulation in vivo. By selecting clones expressing TK-GFP under the control of various promoters, we could use our system for gene expression studies, such as imaging of glucose regulation through the insulin promoter (33), differentiation through the PDX-1 promoter (34), and apoptosis through promoters that respond to activation of NF- κ B, a cellular regulator of cell proliferation and apoptosis (35,36).

Whereas using reporter genes to engineer islets for radionuclide imaging is useful in an experimental setting, it may be possible to implement such an approach in a clinical setting to monitor transplanted islets or the health of endogenous islets. In working toward using a reporter gene approach to image tumor growth in humans, preclinical evaluations of ^{18}F -FHBG have resulted in approval of FHBG for use in clinical trials (37) and protocols for clinical use to detect hepatocellular carcinoma in humans have been published (38).

Another translational approach to detecting endogenous islets lies in the development of targeted radiolabeled probes that can bind to specific cell-surface proteins on the islet or β -cells. In one study, the incretin hormone GLP-1 was conjugated to ^{111}In -1,4,7,10-tetraazacyclododecane- N,N',N'',N''' -tetraacetic acid (DOTA) in an effort to provide a SPECT probe that bound to GLP-1 receptors on the β -cell (39). When administered to rats, all tissues expressing the GLP-1 receptor could be detected by SPECT. Another study (40) showed that ^{11}C -dihydrotrabenazine (DTBZ), a ligand with derivatives suitable for PET, could be used as a probe in a rat model of diabetes to detect changes in β -cell mass before the onset of diabetes. The development of such targeted probes would be ideal for the clinical monitoring of the health of transplanted and endogenous islets.

CONCLUSION

We believe that dual-isotope SPECT combined with engineered islet cells will offer a noninvasive imaging method to follow islet mass and, ultimately, regeneration.

ACKNOWLEDGMENTS

We thank Juri Gelovani for providing the tk gfp plasmid; Paul Picot and Eric Agdeppa for facilitating experiments on the GE specCZT prototype scanner; Jane Sykes and Lela Dorrington for excellent technical assistance with the in vivo experiments; Rennian Wang for assisting with cell transplantations; and Edith Arany and Tom Chrones for immunocytochemistry. Dr. Dhanvantari is a Scholar of the Canadian Diabetes Association and a Scientist of the Alan Thicke Foundation for Juvenile Diabetes. This study was

funded by a Canadian Diabetes Association Grant-in-Aid and a Natural Sciences and Engineering Research Council Discovery Grant.

REFERENCES

- Lu Y, Dang H, Middleton B, et al. Bioluminescent monitoring of islet graft survival after transplantation. *Mol Ther*. 2004;9:428–435.
- Fowler M, Virostko J, Chen Z, et al. Assessment of pancreatic islet mass after islet transplantation using in vivo bioluminescence imaging. *Transplantation*. 2005;79:768–776.
- Gunawardana SC, Hara M, Bell GI, Head WS, Magnuson MA, Piston DW. Imaging beta cell development in real-time using pancreatic explants from mice with green fluorescent protein-labeled pancreatic beta cells. *In Vitro Cell Dev Biol Anim*. 2005;41:7–11.
- Evgenov NV, Medarova Z, Dai G, Bonner-Weir S, Moore A. In vivo imaging of islet transplantation. *Nat Med*. 2006;12:144–148.
- Tai JH, Foster P, Rosales A, et al. Imaging islets labeled with magnetic nanoparticles at 1.5 tesla. *Diabetes*. 2006;55:2931–2938.
- Biancone L, Crich SG, Cantaluppi V, et al. Magnetic resonance imaging of gadolinium-labeled pancreatic islets for experimental transplantation. *NMR Biomed*. 2007;20:40–48.
- Herschman HR. Molecular imaging: looking at problems, seeing solutions. *Science*. 2003;302:605–608.
- Lu Y, Dang H, Middleton B, et al. Noninvasive imaging of islet grafts using positron-emission tomography. *Proc Natl Acad Sci USA*. 2006;103:11294–11299.
- Kim SJ, Doudet DJ, Studenov AR, et al. Quantitative micro positron emission tomography (PET) imaging for the in vivo determination of pancreatic islet graft survival. *Nat Med*. 2006;12:1423–1428.
- Meikle SR, Kench P, Kassiou M, Banati RB. Small animal SPECT and its place in the matrix of molecular imaging technologies. *Phys Med Biol*. 2005;50:R45–R61.
- Stodilka RZ, Blackwood KJ, Kong H, Prato FS. A method for quantitative cell tracking using SPECT for the evaluation of myocardial stem cell therapy. *Nucl Med Commun*. 2006;27:807–813.
- Powers AC, Efrat S, Mojsov S, Spector D, Habener JF, Hanahan D. Proglucagon processing similar to normal islets in pancreatic alpha-like cell line derived from transgenic mouse tumor. *Diabetes*. 1990;39:406–414.
- McGirr R, Ejbick CE, Carter DE, et al. Glucose dependence of the regulated secretory pathway in alphaTC1-6 cells. *Endocrinology*. 2005;146:4514–4523.
- Asfari M, Janjic D, Meda P, Li G, Halban PA, Wollheim CB. Establishment of 2-mercaptoethanol-dependent differentiated insulin-secreting cell lines. *Endocrinology*. 1992;130:167–178.
- Hohmeier HE, Mulder H, Chen G, Henkel-Rieger R, Prentki M, Newgard CB. Isolation of INS-1-derived cell lines with robust ATP-sensitive K^+ channel-dependent and -independent glucose-stimulated insulin secretion. *Diabetes*. 2000;49:424–430.
- Vaidyanathan G, Zalutsky MR. Preparation of 5- ^{131}I iodo- and 5- ^{211}At astato-1-(2-deoxy-2-fluoro-beta-D-arabinofuranosyl) uracil by a halodestannylation reaction. *Nucl Med Biol*. 1998;25:487–496.
- Thyssen S, Arany E, Hill DJ. Ontogeny of regeneration of beta-cells in the neonatal rat after treatment with streptozotocin. *Endocrinology*. 2006;147:2346–2356.
- Lu Y, Dang H, Middleton B, et al. Long-term monitoring of transplanted islets using positron emission tomography. *Mol Ther*. 2006;14:851–856.
- Chen X, Zhang X, Larson CS, Baker MS, Kaufman DB. In vivo bioluminescence imaging of transplanted islets and early detection of graft rejection. *Transplantation*. 2006;81:1421–1427.
- Jin Y, Kong H, Stodilka RZ, et al. Determining the minimum number of detectable cardiac-transplanted ^{111}In -tropolone-labelled bone-marrow-derived mesenchymal stem cells by SPECT. *Phys Med Biol*. 2005;50:4445–4455.
- Slomka PJ, Nishina H, Berman DS, et al. Automatic quantification of myocardial perfusion stress-rest change: a new measure of ischemia. *J Nucl Med*. 2004;45:183–191.
- Kosuda S, Kadota Y, Kusano S, Sekine I. A combined study of Tc-99m Technegas and Xe-133 gas in suspected congenital bronchial atresia. *Clin Nucl Med*. 2003;28:243–244.
- Zhou R, Thomas DH, Qiao H, et al. In vivo detection of stem cells grafted in infarcted rat myocardium. *J Nucl Med*. 2005;46:816–822.
- Brenner W, Aicher A, Eckey T, et al. ^{111}In -Labeled CD34+ hematopoietic progenitor cells in a rat myocardial infarction model. *J Nucl Med*. 2004;45:512–518.

25. Bindslev L, Haack-Sorensen M, Bisgaard K, et al. Labelling of human mesenchymal stem cells with indium-111 for SPECT imaging: effect on cell proliferation and differentiation. *Eur J Nucl Med Mol Imaging*. 2006;33:1171–1177.
26. Muller C, Zielinski CC, Linkesch W, Ludwig H, Sinzinger H. In vivo tracing of indium-111 oxine-labeled human peripheral blood mononuclear cells in patients with lymphatic malignancies. *J Nucl Med*. 1989;30:1005–1011.
27. Zanzonico P, Koehne G, Gallardo HF, et al. [¹³¹I]FIAU labeling of genetically transduced, tumor-reactive lymphocytes: cell-level dosimetry and dose-dependent toxicity. *Eur J Nucl Med Mol Imaging*. 2006;33:988–997.
28. Ogawa K, Harata Y, Ichihara T, Atsushi K, Hashimoto S. A practical method for positron-dependent Compton-scatter correction in single photon emission. *IEEE Trans Med Imaging*. 1991;10:408–412.
29. Kisanuki K, Kishikawa H, Araki E, et al. Expression of insulin receptor on clonal pancreatic alpha cells and its possible role for insulin-stimulated negative regulation of glucagon secretion. *Diabetologia*. 1995;38:422–429.
30. Jensen MV, Joseph JW, Ilkayeva O, et al. Compensatory responses to pyruvate carboxylase suppression in islet beta-cells: preservation of glucose-stimulated insulin secretion. *J Biol Chem*. 2006;281:22342–22351.
31. Efrat S. Genetically engineered pancreatic beta-cell lines for cell therapy of diabetes. *Ann N Y Acad Sci*. 1999;875:286–293.
32. Hohmeier HE, Newgard CB. Islets for all? *Nat Biotechnol*. 2005;23:1231–1232.
33. Hay CW, Docherty K. Comparative analysis of insulin gene promoters: implications for diabetes research. *Diabetes*. 2006;55:3201–3213.
34. Melloul D, Marshak S, Cerasi E. Regulation of pdx-1 gene expression. *Diabetes*. 2002;51(suppl 3):S320–S325.
35. Gross S, Piwnica-Worms D. Real-time imaging of ligand-induced IKK activation in intact cells and in living mice. *Nat Methods*. 2005;2:607–614.
36. Roth DJ, Jansen ED, Powers AC, Wang TG. A novel method of monitoring response to islet transplantation: bioluminescent imaging of an NF- κ B transgenic mouse model. *Transplantation*. 2006;81:1185–1190.
37. Yaghoubi SS, Couto MA, Chen CC, et al. Preclinical safety evaluation of ¹⁸F-FHBG: a PET reporter probe for imaging herpes simplex virus type 1 thymidine kinase (HSV1-tk) or mutant HSV1-sr39tk's expression. *J Nucl Med*. 2006;47:706–715.
38. Yaghoubi SS, Gambhir SS. PET imaging of herpes simplex virus type 1 thymidine kinase (HSV1-tk) or mutant HSV1-sr39tk reporter gene expression in mice and humans using [¹⁸F]FHBG. *Nat Protocols*. 2006;1:3069–3075.
39. Gotthardt M, Lalyko G, van Eerd-Vismale J, et al. A new technique for in vivo imaging of specific GLP-1 binding sites: first results in small rodents. *Regul Pept*. 2006;137:162–167.
40. Souza F, Simpson N, Raffo A, et al. Longitudinal noninvasive PET-based beta cell mass estimates in a spontaneous diabetes rat model. *J Clin Invest*. 2006;116:1506–1513.